Available online at www.sciencedirect.com

ScienceDirect

Procedia Computer Science 48 (2015) 612 – 622

Procedia Computer Science

International Conference on Intelligent Computing, Communication & Convergence

(ICCC-2015)

Conference Organized by Interscience Institute of Management and Technology,

Bhubaneswar, Odisha, India

# VLSI Implementation and analysis of kidney stone detection by Level Set Segmentation and ANN classification

K.Viswanath[a,*], Dr.Gunasundari.R[b], Syed Aathif Hussan[c]

[a,c]*Research Scholar, Pondicherry Engineering College, Department of ECE, Pondicherry,India*
[b]*Associate Professor, Pondicherry Engineering College, Department of ECE, Pondicherry, India*

**Abstract**

The abnormalities of the kidney can be identified by ultrasound imaging. The kidney may have structural abnormalities like kidney swelling, change in its position and appearance. Kidney abnormality may also arise due to the formation of stones, cysts, cancerous cells, congenital anomalies, blockage of urine etc. For surgical operations it is very important to identify the exact and accurate location of stone in the kidney. The ultrasound images are of low contrast and contain speckle noise. This makes the detection of kidney abnormalities rather challenging task. Thus preprocessing of ultrasound images is carried out to remove speckle noise. In preprocessing, first image restoration is done to reduce speckle noise then it is applied to Gabor filter for smoothening. Next the resultant image is enhanced using histogram equalization. Level set segmentation is applied two times, first to segment kidney portion and its output is the input to second to segment stone portion, since it yields better results. In level set segmentation two terms are used in our work. First is using a momentum term and second is based on resilient propagation ($R_{prop}$). Extracted region of the kidney stone after segmentation is applied to Symlets, Biorthogonal (bio3.7, bio3.9 & bio4.4) and Daubechies lifting scheme wavelet subbands to extract energy levels. These energy level gives an indication about presence of stone, which significantly vary from that of normal energy level. These energy levels are trained by Multilayer Perceptron (MLP) and Back Propagation (BP) ANN to identify the type of stone with an accuracy of 98.8% and real time implementation is done using Verilog on Vertex-2Pro FPGA.

* Corresponding author. Tel.: +91-9986278575.
*E-mail address:*viswa_kv@pec.edu


Peer-review under responsibility of scientific committee of International Conference on Computer, Communication and Convergence (ICCC 2015)
doi:10.1016/j.procs.2015.04.143

*Keywords: Kidney Stone database , Level Set Segmentation , Multilayer Perceptron (MLP) and Back Propagation (BP),Lifting Scheme Wavelet transform, Ultrasound imaging, Verilog and FPGA*


Peer-review under responsibility of scientific committee of International Conference on Computer, Communication and Convergence (ICCC 2015)

## 1. Introduction

Kidney stone disease is one of the risks for the life in throughout the world, and majority people with stone formation in kidney initially do not notice it as disease and it damages the limb (organ) slowly. Since kidney malfunctioning can be life threatening, diagnosis of diseases in the earlier stages is crucial. Currently available options include Ultrasound (US) image which is one of the non-invasive low cost, widely used imaging techniques for diagnosing kidney diseases [1]. The Robertson Risk Factor Algorithms (RRFA) are open and are used for laparoscopic surgery, these algorithms are reserved for uncommon [15].Special cases. Hyaluronan is a large (>106 Da) linear glycosaminoglycan composed of repeating units of glucuronic acid (GlcUA) and N-acetyl glucosamine (GlcNAc) disaccharides [16]. Tanzila Rahman, Mohammad Shorif Uddin proposed reduction of speckle noise and segmentation from US image is discussed. It not only detect kidney region, but also enhance image quality [1]. The wan Mahani Hafizah proposed kidney US images were divided into four dissimilar categories: normal, bacterial infection and cystic disease, kidney stones, based on gray level co-occurrence matrix (GLCM) [2]. Gladis Pushpa had proposed Hierarchical Self Organizing Map (HSOM) for brain tumours using segmentation, wavelets packets, and the results were correct up to maximum 97% [3]. Norihiro Koizumi proposed high intensity focused ultrasound (HIFU) technique, used for destroying tumours and stones [4, 13]. K.Viswanath and R. Gunasundari proposed content descriptive of multiple stone detection using level set segmentation, wavelets processing for identification of kidney stone and artificial neural network (ANN) for classification and the results indicate that the maximum accuracy of 98.66% only [5]. The MLP- BP ANN is found as better performance in terms of accuracy having 92%, speed is 0.44 sec and very sensitivity [8, 24]. The Non-invasive combination of renal using pulsed cavitation US therapy proposed shock wave lithotripsy (ESWL) has become a standard for the treatment of calculi located in the kidney and ureter [10]. P.R. Tamilselvi proposed seeded region growing based on segmentation and classification of kidney images with stone sizes using computer aided diagnosis system [31]. Mohammad E. Abou EI-Ghar projected location of urinary stones with unenhanced computed tomography (CT) using half-radiation (low) dose compared with the standard dose and of the 50 patients, 35 patients had a single stone while the rest of them had multiple stones[11]. In order to solve the local minima and segmentation problem the thord Andersson, Gunnar Lathen proposed modified gradient search and level set segmentation [12]. For 3D detection of kidneys and their pathology in real time, the Emmanouil Skounakis proposed *templates based technique* with accuracy of 97.2% and abnormalities in kidneys at an accuracy of 96.1% [13]. For sharpening and smoothening of 2-D image the Gabor function is used to achieve optimal both in time and frequency resolution [25]. Xinjian Chen proposed finite element method based 3-D tumor growth prediction using longitudinal kidney tumor images [30]. For calculation and depth of shock wave scattering by kidney stone in water, the Neil R. Owen proposed pressure finding in fluid by using linear elastic theory [26]. Dirk J. Kok proposed that Prevalence of stone formation due to urinary, Epidemiological is based on pH values [27]. Dinesh S. Datar proposed, the segmentation of required portion is done by initial seed selection, growing and region merging which to not use of any edge detection [28]. Multilayer Perceptron and back propagation implementation on FPGA and ASIC design is carried out by Cyril Prasanna Raj P [29].

This research paper proceeds as follows: In section II problem statement defined, section III describes proposed method, in section IV image segmentation to locate the kidney stone, in section V calculation of energy optimization for segmentation, in section VI wavelets based energy extraction, section VII describes the artificial neural networks classifiers used, in section VIII experiments results are discussion and in the last section we conclude the paper with future work.

## 2. Problem Statement

The kidney malfunctioning can be life threatening, thus detection of kidney stone in the earlier stages is crucial. In order to carry out surgical operation to remove kidney stone it is important to locate the kidney stone. The ultrasound images of kidney contain speckle noise and are of low contrast which makes the detection of kidney abnormalities is a challenging task. As a result the doctors may have problem is to identifying the small kidney stones and their type properly. To address this issue a modified level set segmentation, to identify location of the stone, lifting scheme Wavelets subbands to extract the energy levels of the stone and MLP-BP ANN algorithms for classification is proposed and analyzed [9].

## 3. Methodology

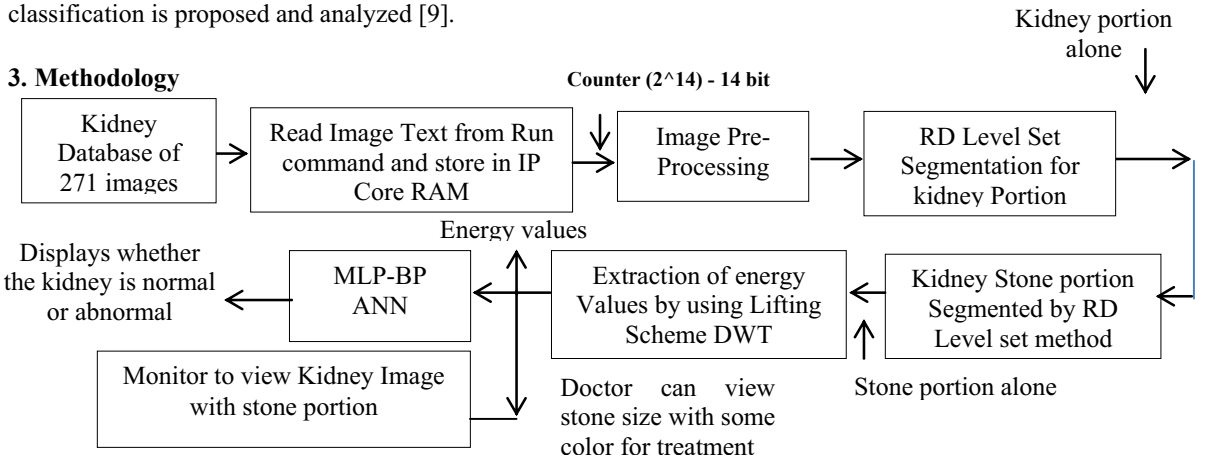


Fig.1. Proposed Block diagram for kidney stone detection

Fig.1. shows the overall block diagram of proposed method. It consists of the following blocks Kidney Image Database, Image Pre-processing, Image Segmentation, Wavelet processing and ANN Classification.

### *3.1. Kidney Image Database*

The 500 US kidney images of both normal and abnormal kidney are collected from different hospitals of different patients and are stored in database. One of the images is taken from the database and subjected to stone detection.

### *3.2. Image Pre-Processing*

The acquired ultrasound (US) image consists of speckle noise and is of low contrast. Due to this, the image quality may not be good for analyzing. For surgical operations it is very important to identify the location of kidney stone. To overcome speckle noise and low contrast, pre-processing of US image needs to be done. Fig.2. shows pre-processing of US image, which consists of the following steps:

1. Image restoration
2. Smoothing and sharpening
3. Contrast enhancement

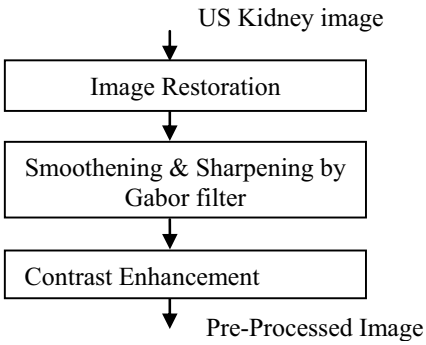


Fig.2. Pre-processing of kidney image

1. *Image Restoration*

The very purpose of image restoration is to reduce the degradations that are caused during acquisition of US scanning. In this system for proper orientation, level set function is used. By the use of plan curve motion, curve smoothers, shrinks are eventually disappeared [1]. Thus Merriman and Sethian proposed evolution between max (k, 0) and min (k, 0).

$$f(x) = \begin{cases} \max(k,0), & if\, a(x,y)x < G(x,y) \\ \min(k,0), & otherwise \end{cases} \qquad \text{----------(1)}$$

Where a(x, y): Average intensity small neighborhood
G(x, y): median in the same neighborhood

*2. Smoothing and Sharpening*

To obtain optimal resolution in both spatial and frequency domains, Gabor filter is used which act as band pass filter for the local spatial frequency distribution [4]. Image smoothing and removal of noise is done by convolution operator. The standard deviation of the Gaussian function can be varied to adjust the degree of smoothening.

*3. Contrast Enhancement*

To improve contrast and to obtain uniform intensity histogram equalization is used. This approach can be used on whole image or part of an image. In this system, enhancing the contrast of the images is done by transforming the values in an intensity image, such that the histogram of the output image approximately matches a specified histogram. The output signal is of same data type as the input signal.

4. **Image Segmentation**

Fig.3. shows the level set segmentation method used first to segment the location of kidney from US scanned image and the segmented kidney portion output is applied again for level set segmentation to segment only stone portion so that processing time will be reduced and image storage memory utilization is also reduces. Proposed work consists of two modified gradient descent methods. First is using a momentum term and second is based on resilient propagation ($R_{prop}$) term. The intention of the segmentation is to overcome difficulties involved in energy function. The energy function depends on properties of the image such as gradients, curvatures, intensities and regularization terms, e.g. smoothing constraints. These are simple, but effective modifications of the basic method are directly compatible with any type of level set implementation. The first proposed method is based on a modification which essentially adds a momentum to the motion in solution space [15, 19]. This simulates the physical properties of momentum and often allows the search to disregard local optima and take larger steps in positive directions. In order to avoid the typical problems of gradient descent search, $R_{prop}$ provides a modification which uses individual adaptive step sizes and the signs of the gradient components.

4.1. *Momentum term*

Spinning to gradient descent with Momentum will adopt the machine learning community and choose a search vector according to: $$a_l = -\eta(1-w)\nabla f_l + w a_{l-1} \qquad ------(2)$$

Where $\eta$ is the *learning rate* and $\omega \in [0, 1]$ is the *momentum*. Note that $w = 0$ gives standard gradient descent $\boldsymbol{a}_l = -\eta\nabla f_l$ , while $w = 1$ gives "infinite momentum" $\boldsymbol{a}_l = \boldsymbol{a}_{l-1}$.

4.2. *$R_{prop}$ term*

The disadvantages of standard gradient descent (SGD) is overcome by incorporating adaptive step-sizes $\nabla_l$ called *update-values* in which each dimension will have one update value i.e. dim $(\nabla_l)$ = dim $(\boldsymbol{x}_l)$. The gradient size is never used in $R_{prop}$. The update rule considers only the signs of the partial derivatives. Another advantage of $R_{prop}$, which is very important in practical use, is the stoutness of its parameters; $R_{prop}$ will work out of the box in many applications using only the standard values of its parameters [18, 20].

We will now describe the $R_{prop}$ algorithm briefly, but for implementation details of $R_{prop}$ we refer to [23, 21]. For $R_{prop}$, we choose a search vector $\boldsymbol{s}_l$ according to: $$s_l = -sign(\nabla f_l) * \nabla_l \qquad ------(3)$$

Where $\nabla_l$ is a vector containing the current update-values and sign $(\cdot)$ the element wise sign function.

4.3. *Energy Optimization for Segmentation*

The segmentation problems can be approached by using the calculus of variations where energy functions is defined representing the objective of the difficulty. The extreme to the functional are found using the Euler-Lagrange equation [10, 22] which is used to derive equations of motion, and the corresponding energy gradients, for the contour [17]. Using these gradients, a gradient descent search in contour space is performed to find a solution to the segmentation problems. Consider, for instance, the derivation of the *weighted region* described by the following functional:

$$f(p) = \iint_{\Omega_p} g(x, y)dxdy \quad -----(4)$$

Where $p$ is a 1D curve embedded in a 2D space, $\Omega_p$ is the region inside of $p$, and $g(x, y)$ is a scalar function. This functional is used to maximize some quantity given by $g(x, y)$ inside $p$. If $g(x, y) = 1$ for instance, the area will be maximized. Calculating the first variation of Eq. 1 yields the evolution equation:

$$\frac{\partial p}{\partial t} = -g(x, y)\eta \quad ----------(5)$$

Where $\eta$ is the curve normal. Using $g(x, y) = 1$ which is constant flow in the negative normal direction. The contour is often implicitly represented by the zero level of a time dependent signed distance function, known as the level set function. The *level set method* was introduced by Osher and Sethian [6]. Formally, a contour $p$ is described by $p = \{\boldsymbol{x}: \varphi(\boldsymbol{x}, t) = 0\}$. The contour $p$ is evolved in time using a set of partial differential equations (PDEs). A motion equation for a parameterized curve $\frac{\partial p}{\partial t} = \gamma\eta$ is in general translated into the level set equation $\frac{\partial \varphi}{\partial t} = \gamma|\nabla\varphi|$ Eq. 2 gives the familiar level set equation: $\frac{\partial \varphi}{\partial t} = -g(x, y)|\nabla\varphi| \quad ------(6)$

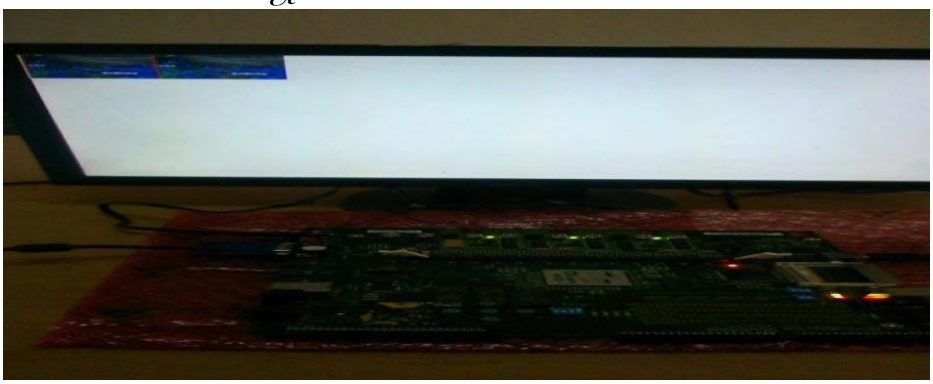

Fig. 3. Level set segmentation of kidney and stone detection on FPGA

In the Fig.3. shows FPGA implementation of kidney stone detection on Vertex-2Pro of device XC2VP30 with 858 inputs and output pins device. The proposed work is design using verilog and configured onto the FPGA board , the output of FPGA is connected to monitor through VGA, the results of first image is kidney portion and second image kidney with stone indicated with red color.

**5. Lifting Scheme Wavelets Processing**

The segmented image (only stone) which has got from previous block is applied to lifting scheme wavelet processing block. It consists of Daubechies filter (Db12), Symlets filter (sym12) and Biorthogonal filter (bio3.7, bio3.9 & bio4.3). *Daubechies filter (Db12)* in this is the number 12 refers to the number of vanishing moments. Basically, the higher the number of vanishing moments, the smoother the wavelet (and longer the wavelet filter) and the length of the wavelet (and scaling) filter is two times that number [3]. *Symlets filter (sym12)* extract features of kidney image and analyse discontinuities and abrupt changes contained in signals, one of the $12^{th}$ - order Symlets wavelets is used. *Biorthogonal filter (bio3.7, bio3.9 & bio4.4)* filter's wavelet energy signatures were considered and averages of horizontal and vertical coefficients details were calculated. Fig.4. shows each filter will give different energy levels or energy features. These energy features will show significant difference, if there is any stone present in the particular region or location. The identification of type of stone is described in next section.

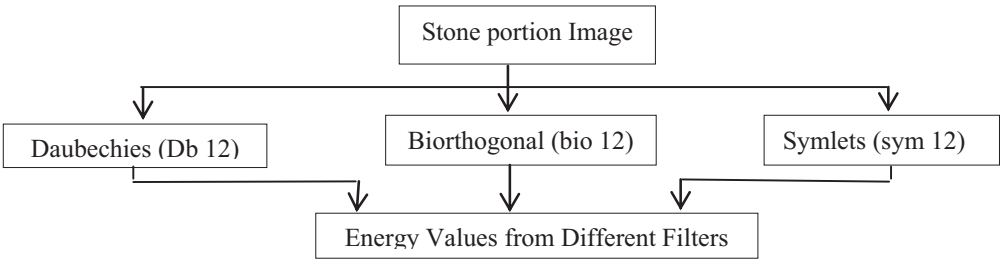


Fig.4. Wavelets filters to extract energy features

In 2-D lifting scheme wavelets transformation consists of update and predictor to get Db12, sym12, bio3.7, bio3.9 and bio4.3 as shown in Fig.5.

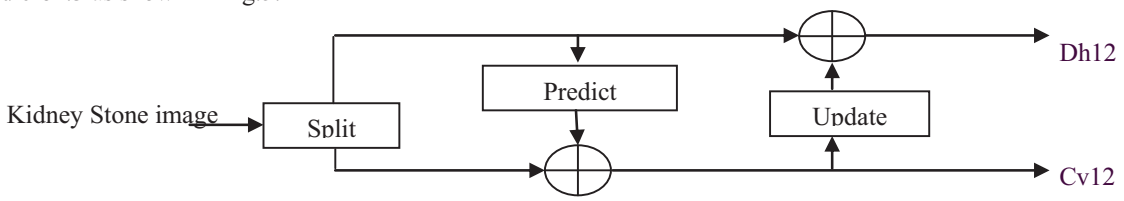


Fig.5. 2-D Lifting Scheme DWT

The equations of predict and update is given by

$$d_i^1=\alpha(x_{2i}+x_{2i+2})+x_{2i+1} \quad --(7) \qquad a_i^1=\beta(d_i^1+d_{i-1}^1)+x_{2i} \quad ------(8)$$

$$d_i^2=\gamma(a_i^1+a_{i+1}^1)+d_i^1 \quad --(9) \qquad a_i^2=\delta(d_i^2+d_{i-1}^2)+a_i^1 \quad -----(10)$$

$$a_i=\varepsilon a_i^2 \quad --(11) \qquad d_i=\frac{d_i^2}{\varepsilon} \quad ----(12)$$

Where $x_{2i}$ and $x_{2i+2}$ are even pixels, $x_{2i+1}$ is odd pixels of stone image and $\alpha,\beta,\gamma,\delta,\varepsilon$ are the constants.

## 6. ANN Classification

In ANN Classification two architectures are used namely, Multilayer Perceptron and back propagation which are described in detail in the following sections.

### *6.1 Multilayer Perceptron (MLP)*

A multilayer perceptron is a feed forward artificial neural network algorithm that maps sets of energy values obtained from wavelets subbands energy extraction shown in the table1. These energy values are fed to input layer and multiplied with initial weights as in equation (13). The back propagation is modified version of linear perceptron in which it uses three or more hidden layers with nonlinear activation function. The back propagation is the most widely applied learning algorithm for multilayer perceptron in neural networks and it employs gradient descent to minimize the squared error between the network output value and desired output value as in equation (14). These error signals are used to calculate the weight updates which represent power of knowledge learnt in the network [7]. Multilayer Perceptron with Back Propagation (MLP-BP) are the main algorithms. Based on the literature survey, MLP-BP algorithm was found to be better than the others in terms of accuracy, speed and performance [14].

The phases involved in ANN are forward phase and backward phase. In back propagation, weights are updated after each pattern and by taking one pattern m at a time as follows:

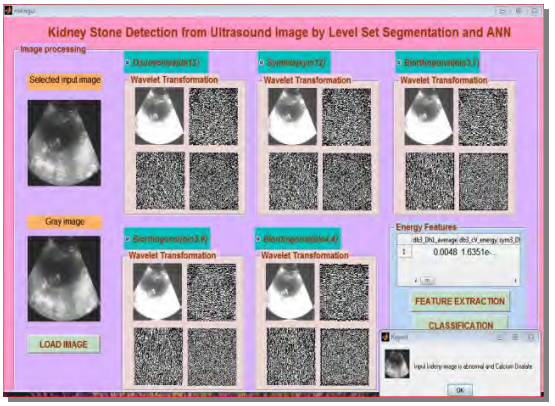


Fig.6. Wavelets subbands energy extraction

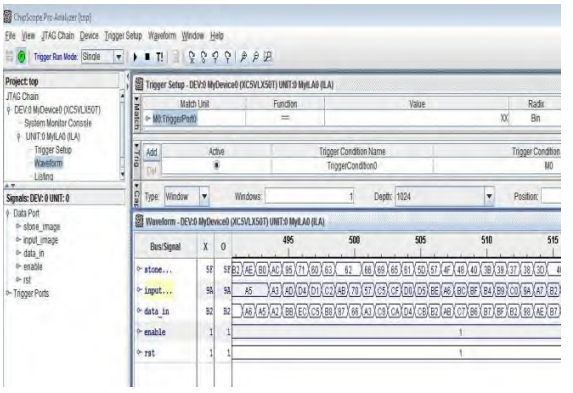

Fig.7. FPGA Hardware implementation using Chipscope, ILA and ICON of segmentation for kidney and stone pixel values

*6.1.1 Forward Phase*

Apply the pattern $X_j^{(l)}$ to the input layer and propagate the signal forward through the network until the final outputs $X_j^L$ have been calculated for each i and L

$$X_j^{(l)} = \theta(s_j^{(l)}) = \theta\left(\sum_{i=0}^{D(L-1)} x_j^{(l)} w_j^{(l)} + w_j^{(l)}\right) \text{------(13)}$$

Where D (L-1) is the number of neurons in layer (L-1), $X_i^{(l-1)}$ output of the $j^{th}$ neuron in the $(l-1)^{th}$ layer, $W_{ij}(i)$ synaptic weight contained in the current neuron, $W_{ij}(i)$ current neuron's bias weight, $X_j^{(l)}$ output of the current neuron.

*6.1.2 Backward Phase*

In this phase, the weights and biases are updated according to the error gradient-descent vector. After an input vector is applied during the forward computation phase, a network output vector is obtained. A target vector t is provided to the network, to drive the network's output toward the expected targeted value [10, 14]. Starting with the output layer, and moving back towards the input layer, calculates the error terms and gradient as follows:

$$e_j^{(l)} = \begin{cases} (1 - x_j^{(l)}) & \text{for} \quad l = L \\ \sum w_{ij}^{(l+1)} s_j^{(l+1)} & \text{for} \quad l = 1,2,3,\ldots\ldots L-1 \end{cases} \text{------(14)}$$

where $e_j^l$ is the error term for $j^{th}$ neuron in the $l^{th}$ layer

$$s_j^{(l=1)} = e_j^{(l+1)} \theta(s_j^{(l)}) \quad \text{for} \quad l = 1,2,\ldots\ldots \text{----(15)}$$

where $\theta(s_j^{(l)})$ is the derivative if the activation function.

Calculate the changes for all the weights as follows:

$$\Delta w_{ij}^{(l)} = \eta s_j^{(l)} x_j^{(l-1)} \ldots\ldots\ldots l = 1,2,\ldots\ldots\ldots L \text{------(16)}$$

where η is the learning rate. Update all the weights as follows:

$$w_{ij}^{(l)}(L+1) = w_{ij}^{(l)}(L) + \Delta w_{ij}^{(l)}(L) \text{------(17)}$$

Where l=1, 2...$L^{(l)}$ and j=0, 1 ...$L^{(l-1)}$, $W_{ij}^{(l)}(L)$ is the current synaptic weight.

$W_{ij}^{(l)}(L+1)$ is the updated synaptic weights to be used in the next feed forward iteration. The Fig.4 show the complete cycle of period, in neural networks training the term period is used to describe a complete pass through all

of the training patterns. The weight in the neural net may be updated after each pattern is presented to the net, or they may be updated just once at the end of the period.

## 7. Implementation and Results

The implementation is done using Verilog on Vertex-2Pro FPGA and simulation results on Matlab 2012A. The Graphical User Interface (GUI) is created from matlab 2012A version and as shown in the Fig.7.From the database of the US kidney images, one kidney image is loaded through the GUI. The loaded image pre-processed and is shown in the GUI. The image segmentation option given in the GUI is selected next to get segmented image. The segmented image is applied for Wavelet processing by selecting one of the lifting wavelet filters shown in the GUI. After selecting the particular filter, that particular wavelet code will be invoked to get resultant image. Then the feature extraction option is selected to get list of energy levels extracted from the segmented image. In the GUI shown in the Fig.6 there is another table which lists energy levels of all the kidney images present in the database. This is done to test the accuracy of MLP-BP ANN system in identifying the kidney images as normal or abnormal and the stone type. Essentially in the database we have both normal and abnormal images which we already know how many of them are normal and abnormal. During the test it is found that our system can classify the kidney images as normal and abnormal almost with accuracy of 98.8% [32]. In Fig.7. is the Chipscope hardware implementation, the first rows shows pixel values of kidney stone, second rows is kidney pixel values and third row is original kidney image.

Table1 shows the lists of energy levels extracted from segmented image. This table is the enlarged version of the table shown in the GUI. The rows of the table are individual energy level of each kidney images of database. The Columns of the table shows energy level extracted from the images of database with respect to each wavelet filter. First two columns are corresponding to Daubechies filter, the third and fourth columns are corresponding to symlets12. The fifth, sixth and seventh columns are corresponding to Biorthogonal filter (Bio3.7). The eighth, ninth and tenth columns are corresponding to Biorthogonal filter (Bio3.9). The eleventh twelfth and thirty columns are corresponding to Biorthogonal filter (Bio4.4).

| Device Utilization Summary | | | |
|---|---|---|---|
| **Slice Logic Utilization** | **Used** | **Available** | **Utilization** |
| Number of Slice Registers | 377 | 28,800 | 1% |
| Number used as Flip Flops | 376 | | |
| Number used as Latches | 1 | | |
| Number of Slice LUTs | 507 | 28,800 | 1% |
| Number used as logic | 424 | 28,800 | 1% |
| Number using O6 output only | 262 | | |
| Number using O5 output only | 119 | | |
| Number using O5 and O6 | 43 | | |
| Number used as Memory | 56 | 7,680 | 1% |
| Number used as Shift Register | 56 | | |
| Number using O6 output only | 55 | | |
| Number using O5 output only | 1 | | |
| Number used as exclusive route-thru | 27 | | |
| Number of route-thrus | 146 | | |
| Number using O6 output only | 146 | | |
| Number of occupied Slices | 235 | 7,200 | 3% |
| Number of LUT Flip Flop pairs used | 617 | | |
| Number with an unused Flip Flop | 240 | 617 | 38% |
| Number with an unused LUT | 110 | 617 | 17% |
| Number of fully used LUT-FF pairs | 267 | 617 | 43% |
| Number of unique control sets | 58 | | |
| Number of slice register sites lost to control set restrictions | 139 | 28,800 | 1% |
| Number of bonded IOBs | 3 | 480 | 1% |
| Number of LOCed IOBs | 3 | 3 | 100% |
| Number of BlockRAM/FIFO | 10 | 60 | 16% |
| Number using BlockRAM only | 10 | | |
| Number of 36k BlockRAM used | 5 | | |
| Number of 18k BlockRAM used | 10 | | |
| Total Memory used (KB) | 360 | 2,160 | 16% |
| Number of BUFG/BUFGCTRLs | 2 | 32 | 6% |
| Number used as BUFGs | 2 | | |
| Number of BSCANs | 1 | 4 | 25% |
| Number of RPM macros | 4 | | |
| Average Fanout of Non-Clock Nets | 3.13 | | |

Fig.8. Design summary of proposed hardware implementation

The proposed work is implemented on Vertex-2Pro FPGA and speed increased by 35% with gate delay of 3.765ns and number of slices LUT's are deceased by 23% as compared to existing methods, the design summary table is shown in Fig.8.

| Db12 Dh1 average | Db12 cV energy | Sym12 Dh1 average | Sym12 cV energy | rbio3.7 Dh1 average | rbio3.7 cD energy | rbio3.7 cV energy | rbio3.7 Dh1 average | rbio3.9 cD energy | rbio3.9 cV energy | rbio3.9 cV average | rbio4.4 Dh1 average | rbio4.4 cH energy |
|---|---|---|---|---|---|---|---|---|---|---|---|---|
| 0.0026 | 5.5953e-05 | 0.0026 | 5.5953e-05 | 0.0052 | 1.3895e-04 | 1.6450e-04 | 0.0043 | 1.0764e-04 | 1.0719e-04 | 0.0039 | 1.7720e-04 | 9.9153e-05 |
| 0.0059 | 7.0192e-05 | 0.0059 | 7.0192e-05 | 0.0127 | 2.2286e-04 | 1.8849e-04 | 0.0128 | 1.7324e-04 | 1.5039e-04 | 0.0129 | 3.9994e-04 | 1.6002e-04 |
| 0.0163 | 9.1629e-04 | 0.0163 | 9.1629e-04 | 0.0316 | 0.0010 | 0.0021 | 0.0306 | 7.6544e-04 | 0.0023 | 0.0303 | 0.0051 | 6.9376e-04 |
| 0.0179 | 3.9806e-04 | 0.0179 | 3.9806e-04 | 0.0255 | 5.4659e-04 | 4.8874e-04 | 0.0263 | 3.9515e-04 | 5.3478e-04 | 0.0267 | 0.0051 | 3.5862e-04 |
| 0.0093 | 2.7436e-04 | 0.0093 | 2.7436e-04 | 0.0249 | 6.8200e-04 | 9.5594e-04 | 0.0214 | 5.2108e-04 | 8.9330e-04 | 0.0198 | 0.0031 | 4.9557e-04 |
| 0.0111 | 9.0990e-04 | 0.0111 | 9.0990e-04 | 0.0239 | 5.5269e-04 | 0.0033 | 0.0197 | 4.1572e-04 | 0.0023 | 0.0179 | 0.0031 | 3.8182e-04 |
| 0.0050 | 1.3049e-04 | 0.0050 | 1.3049e-04 | 0.0094 | 5.6388e-04 | 3.4976e-04 | 0.0087 | 3.9534e-04 | 2.5024e-04 | 0.0085 | 7.2749e-04 | 3.4186e-04 |
| 0.0073 | 7.8642e-05 | 0.0073 | 7.8642e-05 | 0.0136 | 2.6317e-04 | 2.4022e-04 | 0.0132 | 1.8109e-04 | 1.5338e-04 | 0.0133 | 8.1203e-04 | 1.5963e-04 |
| 0.0105 | 2.3515e-04 | 0.0105 | 2.3515e-04 | 0.0137 | 7.1012e-04 | 4.0684e-04 | 0.0131 | 5.2176e-04 | 3.7809e-04 | 0.0133 | 0.0013 | 4.5959e-04 |
| 0.0145 | 1.3983e-04 | 0.0145 | 1.3983e-04 | 0.0154 | 6.6207e-04 | 3.3536e-04 | 0.0144 | 4.8498e-04 | 2.4507e-04 | 0.0184 | 0.0018 | 4.3049e-04 |
| 0.0173 | 2.1550e-04 | 0.0173 | 2.1550e-04 | 0.0278 | 6.2009e-04 | 4.9155e-04 | 0.0262 | 4.7615e-04 | 4.1534e-04 | 0.0260 | 0.0042 | 4.4141e-04 |
| 0.0128 | 3.7797e-04 | 0.0128 | 3.7797e-04 | 0.0256 | 5.8045e-04 | 5.3523e-04 | 0.0234 | 4.5160e-04 | 5.7497e-04 | 0.0238 | 0.0038 | 4.1888e-04 |
| 0.0074 | 0.0018 | 0.0074 | 0.0018 | 0.0132 | 8.6715e-04 | 0.0043 | 0.0133 | 6.7642e-04 | 0.0040 | 0.0140 | 8.5301e-04 | 6.2365e-04 |
| 0.0043 | 2.0368e-04 | 0.0043 | 2.0368e-04 | 0.0072 | 6.4413e-04 | 4.8808e-04 | 0.0066 | 5.2519e-04 | 3.7235e-04 | 0.0065 | 4.2114e-04 | 4.8302e-04 |
| 0.0204 | 3.3482e-04 | 0.0204 | 3.3482e-04 | 0.0379 | 7.3661e-04 | 9.6556e-04 | 0.0353 | 5.1190e-04 | 8.2002e-04 | 0.0344 | 0.0043 | 4.3896e-04 |
| 0.0077 | 0.0012 | 0.0077 | 0.0012 | 0.0169 | 5.8343e-04 | 0.0030 | 0.0158 | 4.5069e-04 | 0.0028 | 0.0153 | 6.8829e-04 | 4.1780e-04 |
| 0.0080 | 1.7951e-04 | 0.0080 | 1.7951e-04 | 0.0161 | 5.8455e-04 | 3.1453e-04 | 0.0155 | 4.8010e-04 | 2.9501e-04 | 0.0154 | 0.0017 | 4.4850e-04 |
| 0.0079 | 2.9445e-04 | 0.0079 | 2.9445e-04 | 0.0151 | 4.5209e-04 | 0.0010 | 0.0134 | 3.6543e-04 | 9.2231e-04 | 0.0126 | 0.0011 | 3.3598e-04 |
| 0.0171 | 5.9446e-04 | 0.0171 | 5.9446e-04 | 0.0325 | 0.0010 | 8.2026e-04 | 0.0214 | 8.0706e-04 | 8.5152e-04 | 0.0180 | 0.0016 | 7.2994e-04 |
| 0.0111 | 1.3944e-04 | 0.0111 | 1.3944e-04 | 0.0224 | 4.9967e-04 | 3.9034e-04 | 0.0211 | 3.9642e-04 | 3.4776e-04 | 0.0202 | 0.0021 | 3.7177e-04 |
| 0.0074 | 2.6753e-04 | 0.0074 | 2.6753e-04 | 0.0153 | 3.5545e-04 | 8.2306e-04 | 0.0141 | 2.8304e-04 | 7.1102e-04 | 0.0136 | 0.0011 | 2.7166e-04 |
| 0.0036 | 2.0845e-04 | 0.0036 | 2.0845e-04 | 0.0065 | 5.9565e-04 | 5.5595e-04 | 0.0061 | 4.5940e-04 | 4.5326e-04 | 0.0061 | 4.0954e-04 | 4.1321e-04 |
| 0.0048 | 1.6351e-04 | 0.0048 | 1.6351e-04 | 0.0083 | 6.4050e-04 | 4.1405e-04 | 0.0086 | 5.0618e-04 | 3.0850e-04 | 0.0085 | 5.2424e-04 | 4.5489e-04 |
| 0.0056 | 8.0388e-05 | 0.0056 | 8.0388e-05 | 0.0106 | 1.5185e-04 | 2.4317e-04 | 0.0115 | 9.1844e-05 | 1.8853e-04 | 0.0139 | 6.2159e-04 | 7.8351e-05 |
| 0.0128 | 2.9260e-04 | 0.0128 | 2.9260e-04 | 0.0255 | 2.4498e-05 | 0.0019 | 0.0272 | 1.0831e-05 | 0.0024 | 0.0258 | 7.3530e-04 | 7.3841e-06 |
| 0.0087 | 6.3554e-04 | 0.0087 | 6.3554e-04 | 0.0157 | 0.0013 | 0.0021 | 0.0143 | 5.8765e-04 | 0.0014 | 0.0146 | 0.0018 | 3.7878e-04 |
| 0.0099 | 8.3973e-04 | 0.0099 | 8.3973e-04 | 0.0123 | 3.7739e-04 | 7.3807e-04 | 0.0163 | 1.9745e-04 | 9.0590e-04 | 0.0189 | 7.7251e-04 | 1.4336e-04 |
| 0.0094 | 0.0011 | 0.0094 | 0.0011 | 0.0219 | 0.0015 | 0.0028 | 0.0239 | 0.0010 | 0.0024 | 0.0247 | 0.0015 | 8.7336e-04 |
| 0.0059 | 2.5405e-04 | 0.0059 | 2.5405e-04 | 0.0112 | 4.3833e-04 | 7.4134e-04 | 0.0105 | 2.6179e-04 | 6.1060e-04 | 0.0105 | 6.9152e-04 | 2.1206e-04 |
| 0.0063 | 7.7728e-04 | 0.0063 | 7.7728e-04 | 0.0124 | 6.3668e-04 | 0.0024 | 0.0112 | 4.0345e-04 | 0.0020 | 0.0109 | 0.0011 | 3.3200e-04 |
| 0.0074 | 8.2789e-04 | 0.0074 | 8.2789e-04 | 0.0152 | 8.4256e-04 | 0.0020 | 0.0128 | 6.0219e-04 | 0.0019 | 0.0118 | 0.0011 | 5.2250e-04 |
| 0.0167 | 4.1325e-04 | 0.0167 | 4.1325e-04 | 0.0156 | 5.3976e-04 | 4.7820e-04 | 0.0140 | 2.9495e-04 | 4.2729e-04 | 0.0136 | 0.0018 | 2.1938e-04 |
| 0.0069 | 5.5092e-04 | 0.0069 | 5.5092e-04 | 0.0122 | 0.0010 | 0.0018 | 0.0113 | 6.9704e-04 | 0.0016 | 0.0119 | 0.0012 | 5.8484e-04 |
| 0.0148 | 9.2528e-04 | 0.0148 | 9.2528e-04 | 0.0298 | 8.8080e-04 | 0.0017 | 0.0214 | 5.8155e-04 | 0.0015 | 0.0163 | 0.0011 | 4.8485e-04 |
| 0.0045 | 2.3998e-04 | 0.0045 | 2.3998e-04 | 0.0080 | 3.3799e-04 | 6.2947e-04 | 0.0069 | 2.5098e-04 | 5.5864e-04 | 0.0065 | 4.1366e-04 | 2.1907e-04 |
| 0.0169 | 0.0011 | 0.0169 | 0.0011 | 0.0336 | 5.8337e-04 | 0.0016 | 0.0241 | 3.8469e-04 | 0.0016 | 0.0182 | 8.5080e-04 | 3.4381e-04 |
| 0.0056 | 8.0388e-05 | 0.0056 | 8.0388e-05 | 0.0106 | 1.5185e-04 | 2.4317e-04 | 0.0115 | 9.1844e-05 | 1.8853e-04 | 0.0139 | 6.2159e-04 | 7.8351e-05 |

Table 1. Energy and average extracted features of all data base kidney images

## 8. Conclusion and Future Work

The proposed work is implemented on Vertex-2Pro FPGA using level set segmentation with momentum and resilient propagation and gives a very effective in identifying the region of stones in the US kidney image with very less utilization of resources. The energy levels extracted from the lifting scheme wavelet subbands i.e. Daubechies (Db12), Symlets (sym12) and Biorthogonal filterers (bio3.7, bio3.9 & bio4.4), gives the clear indication of

difference in the energy levels compared to that of normal kidney image if there is stone. The ANN trained with normal kidney image and classified image input into normal or abnormal by considering extracted energy levels from wavelets filters. The system is tested with different kidney images from database and has classified successfully with the accuracy of 98.8%. So this system can be readily used in the hospitals for detecting abnormality of individuals US kidney image. Thus in this work it is proved that the combination level set segmentation, lifting scheme wavelet filters, multilayer Perceptron with back propagation the better approach for the detection of stones in the kidney. In the future work the system will be designed and implement in real time by placing bio-medical sensors near abdomen to capture kidney portion and captured kidney image is subjected to the proposed algorithm to process and detect stone on FPGA using hardware description language (HDL) and display kidney stone image with colour for easily identification and visibility of stone on monitor.

# References


[1] T.anzila Rahman, Mohammad Shorif Uddin, "Speckle Noise Reduction and Segmentation of Kidney Regions from Ultrasound Image", 978-1-4799-0400-6/13, 2013 IEEE.

[2] Wan Mahani Hafizah, "Feature Extraction of Kidney Ultrasound Images based on Intensity Histogram and Gray Level Co-occurrence Matrix" 2012 sixth Asia Modeling Symposium, 978-0-7695-4730-5/12, 2012 IEEE.

[3] V. P. Gladis Pushpa Rathi, "Detection and Characterization of Brain Tumor Using Segmentation based on HSOM, Wavelet packet feature spaces and ANN", 978-1-4244-8679- 3/11, 2011 IEEE.

[4] Norihiro Koizumi, "Robust Kidney Stone Tracking for a Non-invasive Ultrasound Theragnostic System –Servoing Performance and Safety Enhancement", 2011 IEEE International Conference on Robotics and Automation Shanghai International Conference Center May 9-13, 2011, Shanghai, China.

[5] K.Viswanath and R. Gunasundari, "Kidney stone detection from ultrasound images by Level Set Segmentation and multilayer perceptron ANN", Elsevier publisher, Proceedings of the international Conference on Communication and Comuting , IMCIET-ICCE-2014, pp.38-48, ISBN:978-93-5107-270-6.

[6] S. Osher and J. A. Sethian, "Fronts propagating with curvature dependent speed: Algorithms based on Hamilton– Jacobi formulations," J. Comput. Phys., vol. 79, no. 1, pp. 12–49, Nov. 1988.

[7] M. Stevenson, R. Weinter, and B. Widow, "Sensitivity of Feedforward Neural Networks to Weight Errors" IEEE Transactions on Neural Networks, Vol. 1, No. 2, pp 71-80, 1990.

[8] N.Dheepa "Automatic seizure detection using higher order moments & ANN" IEEE- international conference on advance in Engineering science and management (ICAESM-2012) march 30,31,2012 with ISBN: 978-81-909042-2-3, 2012 IEEE.

[9] Joge Martinez- carballido, "Metamyelocyte nucleus classification uses a set of morphologic templates", 2010 electronics, Robotics and Automatic Mechanics conference 978-0-7695-4204-1/10, 2010 IEE.

[10] P. M. Morse and H. Feshbach, "The variational integral and the Euler equations," in Proc. Meth. Theor. Phys., I, May 1953, pp. 276–280.

[11] Demetrius H. Bagly, Kelly A. Healy, "Ureteroscopic treatment of larger renal calculi (>2cm)", Arab Journal of Urology (2012) 10, 296-300 production and hosting by Elsevier.

[12] William G. Robertson, "Methods for diagnosing the risk factors of stone formation", Arab Journal of Urology (2012) 10, 296-300 production and hosting by Elsevier.

[13] Mohamed E. Abou El-Ghar, "Low-dose unenhanced computed tomography for diagnosing stone disease in obese patients". 2090-598X, 2012 Arab Association of Urolog, Production and hosting by Elsevier B.V, 10,279-283.

[14] M. Riedmiller and H. Braun, "A direct adaptive method for faster backpropagation learning: The RPROP algorithm," in *Proc. IEEE Int. Conf. Neural Netw.*, vol. 1. Jun. 1993, pp. 586–591.

[15] William G Robertson, "Methods for diagnosing the risk factors of stone formation", 2090-598X, 2012 Arab Association of Urolog, Production and hosting by Elsevier B.V, 10,250-257.

[16] Bernhard Hess, "Metabolic syndrome, obesity and kidney stone", 2090-598X, 2012 Arab Association of Urolog, Production and hosting by Elsevier B.V, 10,258-264.

[17] Hyun Wook Park, Todd Schoepflin, "Active Contour model with gradient directional information: Directional Snake", IEEE Transactions on circuits and systems for video technology, Vol.11, No.2, February 2001.

[18] Max W. K. Law and Albert C.S Chung, "Segmentation of Intracranial Vessel and aneurysms in phase contrast magnetic resonance angiography using multirange filters and local variances ", IEEE Transactions on image processing, Vol. 22,No.3,March 2013.

[19] Weidong Zhang, "Mesenteric Vasculature- Guided small Bowel Segmentation on 3-D CT", IEEE Transactions on Medical image, Vol. 32,No.11,Novenber 2013.

[20] Yan Nei Law and Hwee Huan, "A multiresolution Stochastic Level set method for Mumford- shah image segmentation", IEEE Transactions on image processing, Vol. 17,No.12, December 2013.

[21] R. Kimmel, “Fast edge integration,” in Geometric Level Set Methods in Imaging, Vision and Graphics. New York: Springer-Verlag, 2003.
[22] Shijian Lu, Member, IEEE “Automated layer segmentation of optical coherence tomography images”, IEEE Transactions on biomedical engineering, Vol.57, No. 10 October 2010.
[23] Thord Anderrson, Gunnar Lathen, “Modified Gradient search for level set based image segmentation”. IEEE Transactions on image processing, Vol. 22,No.2, February 2013.
[24] Koushal Kumar “Artificial neural network for diagnosis of kidney stone disease”. I.J. Information Technology and Computer Science, 2012,7,20-25.
[25] Linlin Shen and sen Jin “ Three- Dimensional Gabor Wavelets for Pixels- Based Hyperspectral Imagery Classification”, IEEE Transactions on Geoscience and remote sensing, Vol.49, No. 12. December 2011.
[26] Neil R. Owen “Use of acoustic scattering to monitor kidney stone fragmentation during shock wave lithotripsy”, 2006 IEEE Ultrasonics Symposium, 1051-0117/06.
[27] Dirk J. Kok “Metaphylaxis, diet and lifestyle in stone disease”, 2012 Arab Association of urology, Production and hosting by Elsevier B.V, 10, 240-249.
[28] Dinesh S. Datar “Color Image Segmentation based on Initial seed selection, seeded region growing and region merging”, International journal of electronics, Communication & Soft Computing Science and Engineering ISSN 2277-9477, Volume 2 Issue 1.
[29] Cyril Prasanna Raj P “Design and analog VLSI Implementation of Neural Network Architecture for signal Processing”, European Journal of Scientific Research ISSN 1450-216X Vol.27 No.2 (2009),pp.199-216.
[30] Xinjian Chen “FEM-Based 3-D tumor growth prediction for kidney tumor”, IEEE Transactions on biomedical engineering, Vol.58, No.3, March 2011.
[31] P.R. Tamilselvi, “Computer aided diagnosis system for stone detection and early detection of kidney stones”, Journal of Computer Science 7(2):250-254,2011 ISSN 1549-3636.
[32] K.Viswanath and R. Gunasundari, “Design and analysis performance of Kidney Stone Detection from Ultrasound Image by Level Set Segmentation and ANN Classification “,2014 International Conference on Advances in Computing, Communications and Informatics (ICACCI), 978-1-4799-3080-7/14/2014 IEEE, PP 407-414.